10-22-2009

Ferroelectric Polarization Dependent Interactions at Pd-$LiNbO_3$(0001) Interfaces

Mosha H. Zhao
University of Pennsylvania

Dawn A. Bonnell
University of Pennsylvania, BONNELL@SEAS.UPENN.EDU

John M. Vohs
University of Pennsylvania, vohs@seas.upenn.edu

The following article appeared in *Journal of Vacuum Science and Technology.* and may be found at http://dx.doi.org/10.1116/1.3248268.

Ferroelectric Polarization Dependent Interactions at Pd-$LiNbO_3$(0001) Interfaces

Abstract
A combination of Auger electron spectroscopy and temperature-programed desorption was used to characterize the growth and interaction of Pd films with positively and negatively terminated ferroelectric $LiNbO_3$(0001) surfaces. The growth mode of vapor-deposited Pd layers at 300 K was found to be dependent on the direction of the ferroelectric polarization with layer-by-layer growth occurring on the negative ($c-$) surface and particle formation occurring on the positive ($c+$) surface. The Pd metal layers were also found to be more thermally stable on the $c-$ surface relative to the $c+$ surface. These results provide another example of how the polarization orientation in ferroelectric materials affects adsorption and reaction on their exposed surfaces.

Disciplines
Engineering | Materials Science and Engineering

Comments
Suggested Citation:
Zhao, M.H., Bonnell, D.A. and Vohs, J.M. (2009). "Ferroelectric polarization dependent interactions at Pd-$LiNbO_3$(0001) interfaces." *Journal of Vacuum Science and Technology A*. Vol. 27(6).

The following article appeared in *Journal of Vacuum Science and Technology.* and may be found at http://dx.doi.org/10.1116/1.3248268.

Ferroelectric polarization dependent interactions at Pd–$LiNbO_3$(0001) interfaces

Mosha H. Zhao
Department of Chemical and Biomolecular Engineering, University of Pennsylvania, Philadelphia, Pennsylvania 19104

Dawn A. Bonnell
Department of Materials Science and Engineering, University of Pennsylvania, Philadelphia, Pennsylvania 19104

John M. Vohs[a)]
Department of Chemical and Biomolecular Engineering, University of Pennsylvania, Philadelphia, Pennsylvania 19104

(Received 24 July 2009; accepted 21 September 2009; published 22 October 2009)

A combination of Auger electron spectroscopy and temperature-programed desorption was used to characterize the growth and interaction of Pd films with positively and negatively terminated ferroelectric $LiNbO_3$(0001) surfaces. The growth mode of vapor-deposited Pd layers at 300 K was found to be dependent on the direction of the ferroelectric polarization with layer-by-layer growth occurring on the negative ($c-$) surface and particle formation occurring on the positive ($c+$) surface. The Pd metal layers were also found to be more thermally stable on the $c-$ surface relative to the $c+$ surface. These results provide another example of how the polarization orientation in ferroelectric materials affects adsorption and reaction on their exposed surfaces.
 [DOI: 10.1116/1.3248268]

I. INTRODUCTION

Ferroelectric ceramics such as $BaTiO_3$, $LiNbO_3$, and $PbZr_{1-x}Ti_{1-x}O_3$ (PZT) exhibit spontaneous polarization due to a net dipole moment associated with their unit cell. Since their discovery in the 1920s, they have found application in a range electronic and optoelectronic devices[1–3] and the ability to change the direction of the ferroelectric polarization via the application of an external electric field has generated interest in their use in nonvolatile random access memories.[4] It has also been suggested that the ability to manipulate the orientation of the ferroelectric dipole property could be used to tune surface reactivity.[5–16] Several examples indicating that this may indeed be the case have recently appeared in the literature.[5,6,8,9,14–18] For example, the rate of photoreduction of aqueous Ag+ ions[5,6] on $BaTiO_3$ and PZT (Ref. 18) surfaces, and the sticking coefficients and interaction energies of alcohols and water with $BaTiO_3$ (Refs. 14–16) and $LiNbO_3$ surfaces[8,9,12,13] have all been shown to be dependent on the polarization direction.

It has also been suggested that ferroelectric polarization may affect the reactivity of metal films and particles supported on the surface of a ferroelectric oxide and that manipulation of the polarization direction may provide a means to alter their catalytic properties.[17–20] For example, Inoue *et al.*[17] characterized the CO oxidation activity of Pd particles supported on both positively and negatively poled single crystal $LiNbO_3$(0001) substrates. They observed that the activation energy for this reaction was independent of Pd particle size on the negative surface. For thick films on the positive surface, a similar activation energy was observed but decreased substantially for very small particle sizes. They proposed that this decrease may be due to interactions at the Pd–$LiNbO_3$(0001) interface that affects the CO adsorption energy on the Pd. A recent study by Kolpak *et al.*[20] in which density functional theory (DFT) was used to investigate the energetics of adsorption of small molecules, including CO, on Pt films supported on ferroelectric $PbTiO_3$(100) provides some support for the mechanism proposed by Inoue *et al.* The DFT calculations also indicated that for monolayer (ML) Pt films the CO adsorption energies depend on the direction of the polarization in the underlying ferroelectric support.

The results in the study of Inoue *et al.*[17] are interesting and suggest that the direction of the ferroelectric polarization influences the interactions at the Pd–$LiNbO_3$(0001) interface. In the study described here we have investigated this possibility in more detail and have used Auger electron spectroscopy (AES) and CO temperature-programed desorption (TPD) to characterize the structure and thermal stability of vapor-deposited Pd films on both positively and negatively poled $LiNbO_3$(0001) surfaces.

The hexagonal crystal structure of the $LiNbO_3$ lattice is displayed in Fig. 1. The structure lacks inversion symmetry due to displacement of the Nb and Li ions from their centrosymmetric positions thereby making it ferroelectric with a Curie temperature of 1483 K. In this study the bonding of Pd atoms on the positively and negatively terminated (0001) surfaces was studied. The ideal, nonreconstructed structures of these surfaces are shown by the top and bottom planes in Fig. 1. Since the ideal bulk terminations result in charged surfaces, they must either be charge compensated by elec-

a)Electronic mail: vohs@seas.upenn.edu

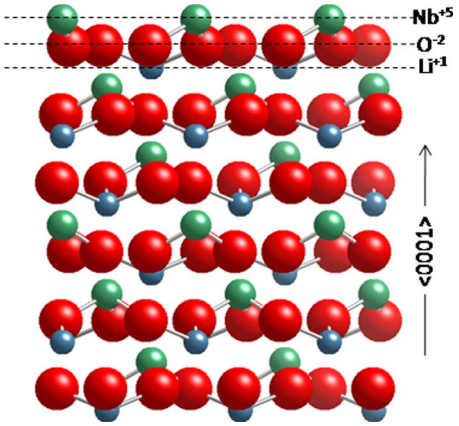

FIG. 1. (Color online) Model of the ferroelectric phase of $LiNbO_3$. The top and bottom planes correspond to the ideal terminations of the (0001) surface.

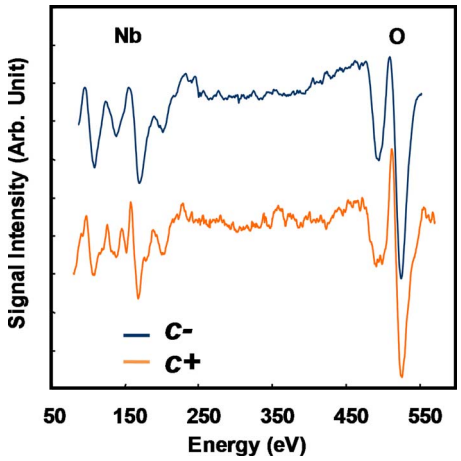

FIG. 2. (Color online) AES spectra of the $c-$ and $c+$ (0001) surfaces of $LiNbO_3$.

trons or holes or undergo reconstruction. The structure and composition of real $LiNbO_3$(0001) surfaces will be discussed below.

II. EXPERIMENTAL PROCEDURES

The $LiNbO_3$(0001) substrates used in this study consisted of $5\times5\times0.5$ mm^2, poled, optical grade, single crystals purchased from MTI. Atomic force microscopy (AFM) (Pacific Nanotechnology Nano-R2) was used to assess the quality of the as received surfaces and they were found to be relatively smooth with a root-mean square roughness of less than 0.5 nm. The poling direction of each crystal was determined by measuring the sign of the pyroelectric voltage that developed across the sample upon heating.[21,22] Following the convention used in previous studies, the positive ($c+$) face corresponds to one that had a negative pyroelectric voltage, and the negative ($c-$) face to the one that had a positive voltage.[9,21]

Experiments were performed using an ultrahigh vacuum chamber (base pressure, 2×10^{-10} torr) equipped with a mass spectrometer (UTI 100C), which was used for TPD experiments, and a cylindrical electron energy analyzer (Omicron) and an electron gun, which were used to collect AES data. The electron beam diameter during the collection of AES spectra was ~1 mm. Prior to introduction into the UHV analysis system, each $LiNbO_3$(0001) sample was ultrasonically cleaned in acetone and then methanol followed by annealing in air at 1173 K for 30 min to reduce the surface carbon contamination. The sample was then soldered to a flat piece of tantalum foil using indium and attached to the UHV sample manipulator. The sample could be heated resistively by passing current through the tantalum foil and the temperature was measured using a type-K thermocouple that was attached to the edge of the sample using a ceramic adhesive. Once in the UHV chamber, the sample was cleaned by sputtering with 2 keV Ar^+ ions followed by annealing at 700 K in 10^{-5} torr of O_2 for 30 min. This procedure was repeated until the amount of surface carbon, the primary contaminant, was below the AES detection limit which is estimated to be less than 0.5% of a monolayer. AFM analysis of samples prepared in this way showed that both the $c+$ and $c-$ terminations had similar morphologies with a rms roughness less than 0.5 nm.

Pd films were deposited using an evaporative Pd source consisting of a short length of 0.127 mm diameter Pd wire (Alfa-Aesar, 99.9%) wrapped around a 0.2 mm diameter tungsten wire, which could be heated resistively. During Pd deposition, the sample was positioned in front of the source and directly above a quartz crystal microbalance (Maxtek TM-100) that was used to monitor the film thickness. Pd thicknesses are reported in equivalent monolayers where 1 ML is defined to be 1.53×10^{15} at./cm^2 which is the surface atom density on Pd(111). CO (Alfa Aesar) was admitted into the vacuum chamber using a variable leak valve and the sample was heated at 1 K/s during all TPD experiments.

III. RESULTS AND DISCUSSION

A. Pd film growth on $LiNbO_3$(0001)

AES was used to characterize the growth of vapor-deposited Pd films on the $c+$ and $c-$ $LiNbO_3$(0001) surfaces. Figure 2 displays the AES spectra of the clean $c+$ and $c-$ surfaces that were prepared by sputtering and annealing in O_2 as described in Sec. II. The spectra contain peaks between 160 and 167 eV due to the Nb(*MNN*) Auger electrons, and between 475 and 550 eV due to O(*KLL*) Auger electrons. The Li(*KLL*) peaks, which should be between 25 and 50 eV, were not resolvable due to a highly sloping background in this region of the spectrum. Note that the spectra for the $c+$ and $c-$ surfaces are nearly identical suggesting that they had similar compositions. The local atomic structure and the types and concentrations of surface defects on each surface, however, may still be dependent on the polarization orientation. The conclusion that the surfaces had similar compositions is consistent with that reported previously by Lushkin *et al.*[23] and Yun *et al.*[24] For example, Lushkin *et al.*[23] also used AES to characterize the composition of $LiNbO_3$(0001) and found that the $c+$ and $c-$ surfaces had similar composi-

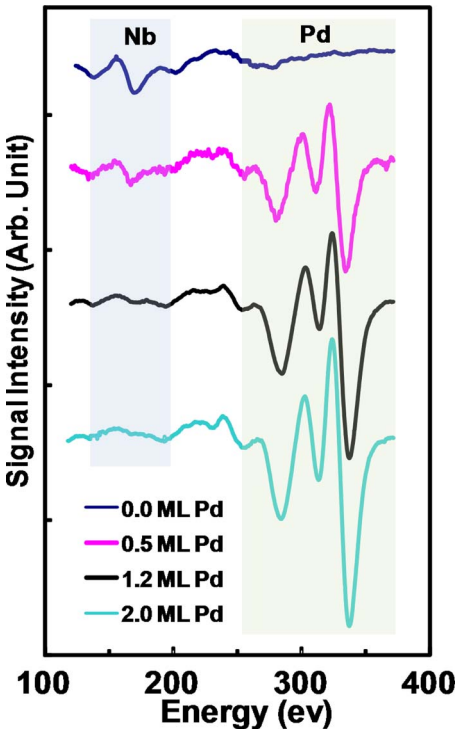

FIG. 3. (Color online) AES spectra of the $c-$ $LiNbO_3$(0001) surface for various Pd coverages.

tion and except for the loss of a small amount of oxygen the composition remained constant for annealing temperatures up to 700 K. For higher annealing temperatures, Li depletion was observed and occurred more rapidly on the $c+$ surface relative to the $c-$ surface. 700 K was used as the annealing temperature in the present study in order to limit the amount of Li desorption.

To determine the growth mode of vapor-deposited Pd films, AES spectra were collected after the deposition of every 0.25 ML of Pd for Pd coverages up to 3 ML. Pd deposition and the AES spectra were collected with sample held at 300 K. A subset of the AES spectra for Pd film growth on the $c-$ $LiNbO_3$(0001) surface is displayed in Fig. 3. Note that the Pd(*MNN*) peaks appear between 280 and 330 eV. As expected the peak-to-peak amplitude of the primary Pd(*MNN*) peak increases with Pd coverage while that of the Nb(*MNN*) peak decreases. The amplitudes of the Pd(*MNN*) and Nb(*MNN*) peaks as a function of the amount of Pd deposited for all of the spectra collected in the series are displayed in Fig. 4(a). A similar data set for the growth of a Pd film on the $c+$ $LiNbO_3$(0001) surface is presented in Fig. 4(b). Note that the values reported in this figure have been corrected to account for differences in the cross sections for emission of the Auger electrons from each element using sensitivity factors reported in the literature.[25]

The shapes of the curves for the Pd(*MNN*) and Nb(*MNN*) peaks in Fig. 4 provide insight into the growth mode of the Pd films.[26–28] Note that the data for the $c-$ $LiNbO_3$(0001) surface [Fig. 4(a)] show that the Pd(*MNN*) signal increases rapidly with coverage, while that for Nb(*MNN*) decreases rapidly and asymptotically approaches zero for Pd coverages greater than 3 ML. This behavior suggests that the Pd film grows in a layer-by-layer fashion (i.e., Frank–van der Merwe growth[27]). To confirm that this was indeed the case, the experimental results were compared to predictions based on both discrete and continuum-based models of film growth. In the discrete model, one accounts for adsorption of individual Pd atoms on the surface. For layer-by-layer growth during deposition of the first monolayer, the AES signal for the Pd will increase linearly with Pd coverage since each additional atom will contribute an equal amount to the signal. A linear relationship is also expected to occur for the second monolayer except that the slope will be less since each additional Pd atom also causes some attenuation of the signal from the first layer atoms. The slope will decrease with subsequent monolayers and ultimately go to zero when the thickness of the Pd film is equal to the AES sampling depth. A similar trend, except with opposite slopes, would be expected for the AES signal from the substrate. The data in Fig. 3 for the $c-$ $LiNbO_3$(0001) surface exhibit trends consistent with this model. As shown by the solid lines in the figure, there is a

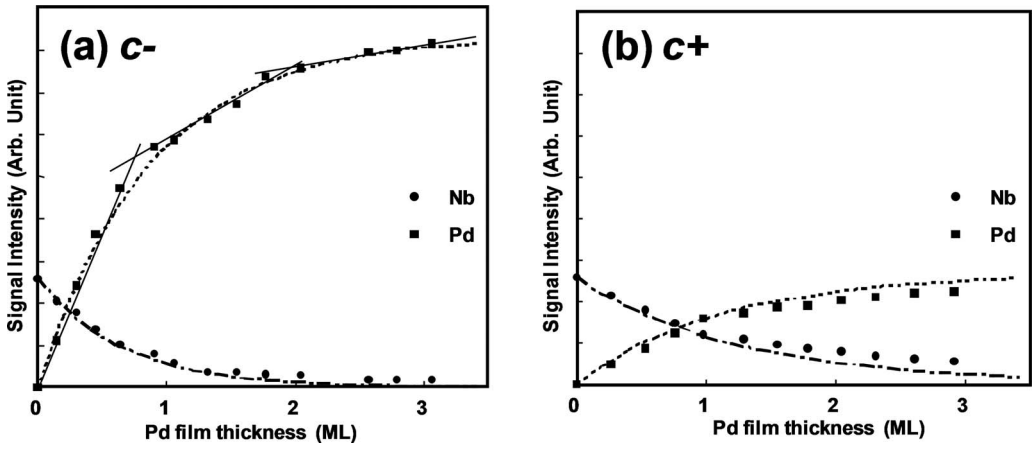

FIG. 4. Peak-to-peak intensities of the of Nb and Pd AES signals as a function of the Pd coverage for (a) $c-$ and (b) $c+$ $LiNbO_3$(0001). The solid and dashed lines are best fits to discrete and continuum models of layer by-layer growth, respectively. The same arbitrary units are used in parts (a) and (b).

linear relationship between the Pd(*MNN*) signal and the Pd coverage with changes in slope that occur near 1 and 2 ML (the 1–2 ML transition occurs slightly below 1 ML which may be due to the uncertainty in the measurement of the amount of Pd deposited). This result indicates that the Pd film grows in a layer-by-layer fashion on the *c*− surface.

Comparisons to predictions based on a continuum model[29,30] further support the conclusion that the Pd film grows layer-by-layer on *c*− $LiNbO_3$(0001). Using the model proposed by Gallon[29] for layer-by-layer growth, the AES signal intensity of *n*th layer of Pd atoms, I_n^{Pd}, is given by the following equation:

$$I_n^{Pd} = I_\infty^{Pd}\left[1 - \left(1 - \frac{I_1^{Pd}}{I_\infty^{Pd}}\right)^n\right], \quad (1)$$

where I_∞^{Pd} is the intensity obtained from a Pd film that is thicker than the AES sampling depth. Using values of I_∞^{Pd} and I_1^{Pd} obtained from the experimental data, this equation can be used to predict the entire I^{Pd} versus Pd coverage curve. This is a continuum model because it assumes that noninteger Pd coverages consist of a uniform film over the entire surface, e.g., a 0.5 ML film is modeled as a continuous film that has a thickness equal to one-half that of a monolayer film. The AES signal intensity for the Nb in the $LiNbO_3$ substrate after depositing *n* layers of Pd, I_n^{Nb}, is given by

$$I_n^{Nb} = I_0^{Nb}\left(\frac{I_1^{Nb}}{I_0^{Nb}}\right)^n, \quad (2)$$

where the values of I_n^{Nb} and I_1^{Nb} are again determined form the experimental data.

The curves for the AES intensities as a function of the Pd coverage predicted by Eqs. (1) and (2) are displayed as the dashed lines in Fig. 4. Note that for the *c*− $LiNbO_3$(0001) surface [Fig. 4(a)], there is an excellent agreement between the experimental data and the simulated growth curves. This again demonstrates that the AES data for Pd on *c*− $LiNbO_3$(0001) exhibits trends that are consistent with layer-by-layer growth of the Pd film.

The changes in the AES peak intensities for the *c*+ $LiNbO_3$(0001) surface [Fig. 4(b)] as a function of the Pd coverage are much less pronounced than those for the *c*− surface. Note that the intensity of the Pd(*MNN*) peak for the as-deposited 3 ML film on the *c*+ surface is less than one-third of the value for the *c*− surface. This result demonstrates that the vapor-deposited Pd on this surface forms three-dimensional particles (i.e., Volmer–Weber growth) at 300 K. The growth curves for *c*+ $LiNbO_3$(0001) also cannot be adequately fit using Eqs. (1) and (2). The dashed lines in the figure correspond to the predictions based on these equations using the data points at 1 ML Pd to determine the values for I_1^{Pd} and I_1^{Nb}. Note that for the higher coverages the predicted values are all higher than the measured values for Pd(*MNN*) and lower for Nb(*MNN*). This result is again consistent with the conclusion that the Pd forms particles at 300 K on the *c*+ $LiNbO_3$(0001) surface.

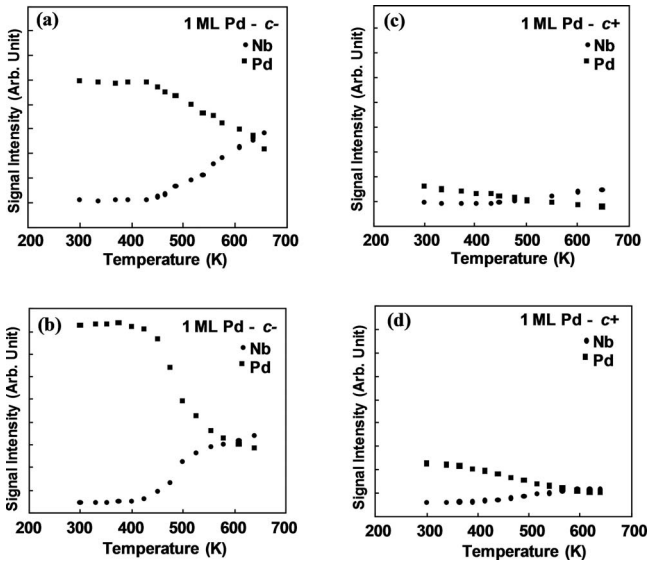

FIG. 5. Peak-to-peak intensities for the Pd and Nb AES signals as a function of the annealing temperature for (a) 1 ML of Pd on the *c*− surface, (b) 3 ML of Pd on the *c*− surface, (c) 1 ML of Pd on the *c*+ surface, and (d) 3 ML of Pd on the *c*+ surface. The same arbitrary units are used in each plot.

B. Influence of ferroelectric polarization on Pd film stability

The thermal stability of the Pd layers on the *c*+ and *c*− $LiNbO_3$(0001) surfaces was also investigated by monitoring the Nb(*MNN*) and Pd(*MNN*) AES signals for 1 and 3 ML Pd films as a function of the sample annealing temperature. The results of these experiments are displayed in Fig. 5. Note that in these experiments the sample was heated to the indicated temperature and then allowed to cool back to room temperature at which point the AES data were collected.

The thermal stability data for the 1 and 3 ML Pd films on the *c*− surface exhibit similar trends. In both cases for annealing temperatures up to 425 K, the Nb(*MNN*) and Pd(*MNN*) AES peaks remain nearly constant indicating no major changes in the morphology of the Pd film. Heating to higher temperatures, however, caused a rapid decrease in the intensity of the Pd(*MNN*) peak with a concomitant increase in the Nb(*MNN*) peak. For the 3 ML Pd film, the peak intensities level out at temperatures above 575 K. These results indicate that the continuous Pd film is stable on the *c*− surface up to 425 K at which point it starts to agglomerate into particles and that this agglomeration process in nearly complete by 575 K. The analogous data for the *c*+ surface does not exhibit a stable region at low temperatures and the Pd(*MNN*) peak starts to decrease upon heating above room temperature. This result demonstrates that the Pd particles that are formed on this surface at room temperatures have low thermal stability and further agglomerate into larger particle upon heating.

CO TPD was also used to characterize 1 ML Pd films on the *c*+ and *c*− $LiNbO_3$(0001) surfaces and the data obtained in these studies are summarized in Figs. 6 and 7. In these experiments the sample was dosed to saturation with CO at 250 K. In TPD experiments performed prior to Pd deposition

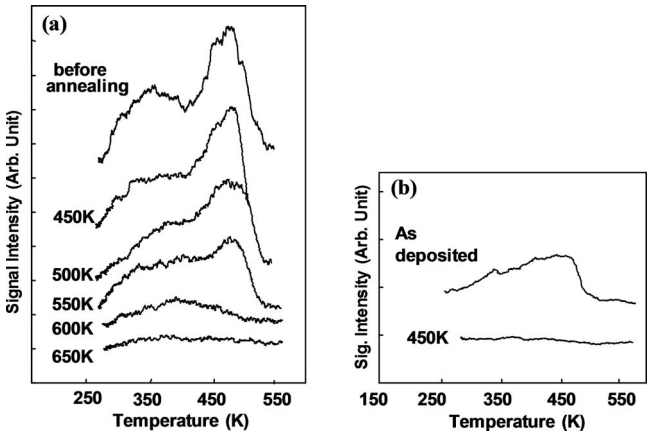

FIG. 6. CO TPD spectra obtained from (a) $c-$ and (b) $c+$ 1 ML Pd/$LiNbO_3$(0001) samples as a function of the annealing temperature.

it was found that CO does not adsorb on both the $c+$ and $c-$ surfaces at temperatures above 150 K. Thus, the peaks in the TPD spectra in Fig. 6 can be attributed to CO desorbing form the Pd.

Figure 6(a) displays CO TPD data obtained from the 1 ML Pd $c-$ $LiNbO_3$(0001) sample. The top spectrum in the figure was obtained from a freshly deposited 1 ML Pd film and contains a relatively narrow peak centered at 490 K and a much broader and less intense peak centered at 360 K. These features are consistent with those reported for Pd(111) (Refs. 31–33) and supported Pd particles.[34] The low- and high-temperature peaks can be assigned to CO adsorbed in Pd bridge and Pd threefold sites, respectively.[31,32] The remaining spectra in this figure were obtained from samples that had been annealed to the indicated temperature after Pd deposition but prior to CO exposure. Note that only minor differences in the spectra are observed for annealing temperatures up to 450 K. For higher annealing temperatures, however, the area of the CO peaks decrease with the area of the high-temperature peak decreasing more rapidly than that of the low-temperature peak. The total area of the CO peaks as a function of the annealing temperature following Pd deposition is plotted in Fig. 7. The CO peak area provides an estimate of the surface area of the Pd. Note that for the $c-$ surface the trend in the CO peak area with annealing temperature is similar to that exhibited by the Pd(*MNN*) Auger peak. The CO TPD data therefore further support the conclusion that Pd films on $c-$ $LiNbO_3$(0001) are stable up to ~450 K at which point they start to agglomerate into particles.

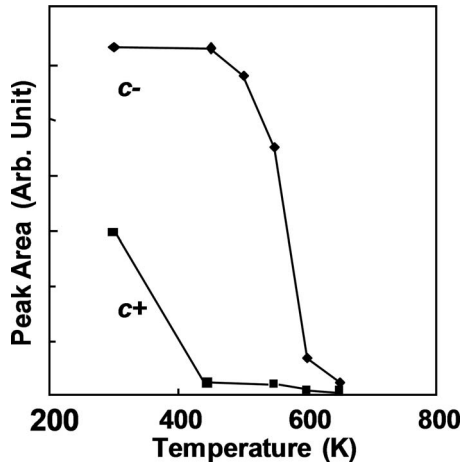

FIG. 7. CO TPD peak areas for $c-$ and $c+$ 1 ML Pd/$LiNbO_3$(0001) samples as a function of the annealing temperature.

As expected based on the AES results, the area of the CO TPD peaks from a freshly deposited 1 ML Pd film on $c+$ $LiNbO_3$(0001) was much less than that from the corresponding $c-$ $LiNbO_3$(0001) surface [see Figs. 6(b) and 7]. Preannealing the 1 ML Pd $c-$ $LiNbO_3$(0001) sample to 450 K resulted in the near disappearance of the CO TPD peaks indicating the loss of most of the exposed Pd atoms. These results are again consistent with the AES results and show that the as deposited Pd forms particles on $c+$ $LiNbO_3$(0001) and that these particles are not thermally stable and undergo rapid agglomeration upon heating.

Together the AES and CO TPD results show that the orientation of the ferroelectric dipoles has a dramatic effect on the interaction of Pd with $LiNbO_3$(0001). Pd interacts strongly with the $c-$ surface and vapor-deposited Pd grows in a layer-by-layer fashion at 300 K. Pd films on the $c-$ surface are stable up to ~425 K at which point they agglomerate into particles. In contrast, Pd interacts only weakly with the $c+$ surface. On this surface, vapor-deposited Pd forms particles at 300 K which agglomerate into larger particles upon heating. While the orientation of the ferroelectric dipoles clearly affects the strength of the Pd–$LiNbO_3$(0001) interaction, further study is needed in order to determine the mechanism by which polarization affects the bonding interactions. It is possible; however, that changes in the surface structure, composition, and electronic properties all play a role.

As noted above, the AES results obtained in this study and those reported previously by Lushkin *et al.*[23] indicate that the $c+$ and $c-$ surfaces have similar compositions. This conclusion is consistent with a more detailed study of the surface structure of $LiNbO_3$(0001) reported by Yun *et al.*[24] In that study based on x-ray photoelectron spectroscopy (XPS), ion scattering spectroscopy (ISS), and TPD data, it was also concluded that the $c+$ and $c-$ surfaces prepared by annealing in oxygen in UHV had similar compositions and both exhibited (1×1) low energy electron diffraction patterns indicating that they had similar structures. As noted by Yun *et al.*, this result is somewhat surprising since one might expect these surfaces to reconstruct in order to stabilize the divergent electric field produced by the ordered ferroelectric dipoles in the bulk of the crystal. In order to account for the required screening of the electric field, they proposed an adatom/vacancy model. In this model, on one surface of the crystal oxygen, adatoms cover the exposed Nb atoms, while on the opposing surface Li and O atoms are exposed. They were unable to unambiguously assign these surface structures to the $c+$ or $c-$ terminations, but based on the presence

of a small shoulder on the O(1*s*) XPS peak they speculated that the oxygen adatom/Nb surface may be the *c*− termination. Unfortunately these proposed differences in surface structure cannot be discerned by XPS and AES due to their sampling depth, and since ISS is insensitive to Li both surfaces appear to be completely oxygen terminated by this technique. It is noteworthy, however, that based on these proposed differences in surface composition, one might expect adsorbed Pd atoms to interact differently with the two surfaces. Thus, this model provides at least one plausible explanation for the results obtained in the present study.

A recent theoretical study by Levchenko and Rappe[35] also provides useful insights into the possible origins of the different interaction energies for Pd with the *c*+ and *c*− $LiNbO_3$(0001) surfaces. In that study, DFT methods were used to calculate the relative stability of the *c*+ and *c*− surfaces and to predict changes in the surface composition for a range of temperatures and oxygen pressures. Their calculations indicated that there are significant differences in the equilibrium composition of the *c*+ and *c*− surfaces and that stabilization of the surface charge resulting from the ferroelectric polarization is achieved primarily by these compositional changes rather than by mobile charge carries (i.e., passivation with ions is favored over passivation with electrons or holes), and that the *c*+ surface contains more O and Li than the *c*− surface. These predictions are consistent with the results of Yun *et al.*[24] and both the theoretical and experimental studies indicate that small differences in the surface composition play an important role in stabilizing the surface charge. The Levchenko and Rappe study therefore also suggest that differences in the composition of the *c*+ and *c*− surfaces may be responsible for the different interaction energies of Pd with each surface.

IV. SUMMARY

The AES and CO TPD data obtained in this study demonstrate that at 300 K vapor-deposited Pd films grow in a layer-by-layer fashion on the *c*− $LiNbO_3$(0001) surface. In contrast on the on the *c*+ $LiNbO_3$(0001) surface, the Pd forms three-dimensional clusters for identical growth conditions. These differences can be attributed to differences in the interaction energy of Pd with the *c*− and *c*+ surfaces. This conclusion is supported by thermal stability studies which showed that Pd films on the *c*− surface are stable up to ~425 K at which point they start to agglomerate into particles, while particle formation occurs upon Pd deposition at 300 K on the *c*+ surface. Previous studies of the structure and composition of the *c*− and *c*+ $LiNbO_3$(0001) suggest that the differences in the bonding at the Pd–$LiNbO_3$ interfaces is likely to be due to differences in the composition of *c*− and *c*+ surfaces.

ACKNOWLEDGMENTS

We gratefully acknowledge support of this work by the NSF MRSEC program (Grant No. DMR05-20020) and would like to thank Penn's Nano/Bio Interface Center for the use of its facilities.

[1] J. M. Herbert, *Ferroelectric Transducers and Sensors* (Gordon and Breach Science, New York, 1982).
[2] J. F. Scott, Science **315**, 954 (2007).
[3] R. C. Buchanan, *Ceramic Materials for Electronics: Processing, Properties and Applications* (Dekker, New York, 1986).
[4] R. E. Jones, P. D. Maniarb, R. Moazzamic, P. Zurchera, J. Z. Witowskid, Y. T. Liib, P. Chua, and S. J. Gillespie, Thin Solid Films **270**, 584 (1995).
[5] J. L. Giocondi and G. S. Rohrer, Chem. Mater. **13**, 241 (2001).
[6] J. L. Giocondi and G. S. Rohrer, J. Phys. Chem. B **105**, 8275 (2001).
[7] G. Parravano, J. Chem. Phys. **20**, 342 (1952).
[8] Y. Yun and E. I. Altman, J. Am. Chem. Soc. **129**, 15684 (2007).
[9] Y. Yun, L. Kampschulte, M. Li, D. Liao, and E. I. Altman, J. Phys. Chem. C **111**, 13951 (2007).
[10] A. L. Cabrera, F. Vargas, and J. J. Albers, Surf. Sci. **336**, 280 (1995).
[11] A. L. Cabrera, B. C. Sales, M. B. Maple, H. Suhl, G. W. Stupian, and A. B. Chase, Mater. Res. Bull. **14**, 1155 (1979).
[12] J. Garra, J. M. Vohs, and D. A. Bonnell, J. Vac. Sci. Technol. A **27**, L13 (2009).
[13] J. Garra, J. M. Vohs, and D. A. Bonnell, Surf. Sci. **603**, 1106 (2009).
[14] M. H. Zhao, D. A. Bonnell, and J. M. Vohs, Surf. Sci. **602**, 2849 (2008).
[15] D. B. Li, M. H. Zhao, J. Garra, A. M. Kolpak, A. M. Rappe, D. A. Bonnell, and J. M. Vohs, Nature Mater. **7**, 473 (2008).
[16] M. H. Zhao, D. A. Bonnell, and J. M. Vohs, Surf. Sci. **603**, 284 (2009).
[17] Y. Inoue, I. Yoshioka, and K. Sato, J. Phys. Chem. **88**, 1148 (1984).
[18] D. Li and D. A. Bonnell, Ceram. Int. **34**, 157 (2008).
[19] Y. Inoue, M. Matsukawa, and K. Sato, J. Phys. Chem. **96**, 2222 (1992).
[20] A. M. Kolpak, I. Grinberg, and A. M. Rappe, Phys. Rev. Lett. **98**, 166101 (2007).
[21] G. D. Boyd, K. Nassau, R. C. Miller, W. L. Bond, and A. Savage, Appl. Phys. Lett. **5**, 234 (1964).
[22] R. S. Weis and T. K. Gaylord, Appl. Phys. A: Mater. Sci. Process. **37**, 191 (1985).
[23] A. Y. Lushkin, V. B. Nazarenko, K. N. Pilipchak, V. F. Shnyukov, and A. G. Naumovets, J. Phys. D **32**, 9 (1999).
[24] Y. Yun, M. Li, D. Liao, L. Kampschulte, and E. I. Altman, Surf. Sci. **601**, 4636 (2007).
[25] L. Davis, N. MacDonald, P. Palmberg, G. Riach, and R. Weber, *Handbook of Auger Electron Spectroscopy, a Reference Book of Standard Data for Identification and Interpretation of Auger Electron Spectroscopy Data* (Perkin-Elmer Corporation, Eden Prairie, MN, 1976).
[26] M. P. Seah, Surf. Sci. **32**, 703 (1972).
[27] J. A. Venables, G. D. T. Spiller, and M. Hanbucken, Rep. Prog. Phys. **47**, 399 (1984).
[28] D. N. Belton, Y.-M. Sun, and J. M. White, J. Phys. Chem. **88**, 1690 (1984).
[29] T. E. Gallon, Surf. Sci. **17**, 486 (1969).
[30] C. Argile and G. E. Rhead, Surf. Sci. Rep. **10**, 277 (1989).
[31] W. K. Kuhn, J. Szanyi, and D. W. Goodman, Surf. Sci. Lett. **274**, L611 (1992).
[32] X. Guo and J. John T. Yates, J. Chem. Phys. **90**, 6761 (1989).
[33] D. I. Jerdev, R. Prins, and B. E. Koel, J. Phys. Chem. B **108**, 14417 (2004).
[34] H. Cordatos, T. Bunluesin, and R. J. Gorte, Surf. Sci. **323**, 219 (1995).
[35] S. V. Levchenko and A. M. Rappe, Phys. Rev. Lett. **100**, 256101 (2008).